Ectodysplasin Signaling through XEDAR Is Required for Mammary Gland Morphogenesis

JID Open

Abigail R. Wark[1], Daniel Aldea[2,3], Reiko R. Tomizawa[1,3], Blerina Kokalari[2], Bailey Warder[2] and Yana G. Kamberov[2]

XEDAR is a member of the TNF receptor subfamily and a mediator of the ectodysplasin (EDA) pathway. EDA signaling plays evolutionarily conserved roles in the development of the ectodermal appendage organ class, which includes hair, eccrine sweat glands, and mammary glands. Loss-of-function sequence variants of *EDA*, which encodes the two major ligand isoforms, EDA-A1 and EDA-A2, result in X-linked hypohidrotic ectodermal dysplasia characterized by defects in two or more types of ectodermal appendages. EDA-A1 and EDA-A2 signal through the receptors EDAR and XEDAR, respectively. Although the contributions of the EDA-A1/EDAR signaling pathway to EDA-dependent ectodermal appendage phenotypes have been extensively characterized, the significance of the EDA-A2/XEDAR branch of the pathway has remained obscure. In this study, we report the phenotypic consequences of disrupting the EDA-A2/XEDAR pathway on mammary gland differentiation and growth. Using a mouse *Xedar* knockout model, we show that *Xedar* has a specific and temporally restricted role in promoting late pubertal growth and branching of the mammary epithelium that can be influenced by genetic background. Our findings implicate *Xedar* in ectodermal appendage development and suggest that the EDA-A2/XEDAR signaling axis contributes to the etiology of *EDA*-dependent mammary phenotypes.

Journal of Investigative Dermatology (2023) **143,** 1529–1537; doi:10.1016/j.jid.2023.02.007

INTRODUCTION

The ectodysplasin (EDA) signaling pathway has long been recognized for its pivotal role in the development, pattering, and differentiation of mammalian ectodermal appendages, including hair follicles, eccrine sweat glands, teeth, and mammary glands (Biggs and Mikkola, 2014; Cui et al., 2014, 2009; Headon et al. 2001; Headon and Overbeek, 1999; Lindfors et al., 2013; Tucker et al., 2000; Voutilainen et al., 2015, 2012; Wahlbuhl et al., 2018; Wahlbuhl-Becker et al., 2017). Alternative splicing of transcripts encoded by the anhidrotic ectodermal dysplasia gene *EDA* produces two main protein isoforms, EDA-A1 and EDA-A2, which belong to the TNF ligand superfamily (Yan et al., 2000). An insertion of two amino acids differentiates the EDA-A1 isoform from the isoform EDA-A2 and is necessary and sufficient to confer exclusive binding to the receptors EDAR and XEDAR, respectively (Yan et al., 2000). EDAR and XEDAR are type III transmembrane receptors whose respective binding to EDA-A1 and EDA-A2 oligomers has been shown to activate downstream NF-kB signaling and, in some contexts, c-Jun N-terminal kinase signaling (Kumar et al., 2001; Sinha and Chaudhary, 2004; Yan et al., 2000).

In humans, loss-of-function sequence variants of *EDA* are causal to the majority of cases of the most common form of ectodermal dysplasia, X-linked hypohidrotic ectodermal dysplasia (XLHED) (number MIM 305100) (Cluzeau et al., 2011). Affected individuals present with clinical features in two or more ectodermal appendages, including reduced numbers or total loss of eccrine glands; sparse hair; missing teeth; and mammary phenotypes, including impaired breast and nipple development and lactation difficulties in females (Cluzeau et al., 2011; Wahlbuhl-Becker et al., 2017). The role of *EDA* in ectodermal appendage development is evolutionarily conserved. The two widely studied tabby loss of function alleles of the murine *Eda* locus, $Eda^{Ta\text{-}6J}$ and Eda^{Ta}, which harbor a frameshift-inducing base pair deletion and a deletion in exon 1, respectively, cause highly homologous ectodermal appendage defects to those of human patients with XLHED (Biggs and Mikkola, 2014; Cui and Schlessinger, 2006; Mikkola and Thesleff, 2003; Sofaer and MacLean, 1970; Srivastava et al., 1997; Wahlbuhl et al., 2018). These phenotypes, particularly in hair follicles and eccrine glands, are thought to result from the disruption of the EDA-A1/EDAR signaling axis because loss-of-function sequence variants in *Edar* largely phenocopy the defects observed in $Eda^{Ta\text{-}6J}$ and Eda^{Ta} mutants, and exogenous treatment with recombinant EDA-A1 protein rescues or improves many of the XLHED hair and eccrine phenotypes in mice, humans, and dogs (Casal et al., 2007; Gaide and Schneider, 2003; Margolis et al., 2019; Mustonen et al., 2004, 2003; Schneider et al., 2018; Srivastava et al., 2001). In contrast, the extent to which the EDA-A2/XEDAR signaling axis contributes to *EDA*-dependent ectodermal appendage phenotypes is unclear.

[1]*Department of Genetics, Harvard Medical School, Boston, Massachusetts, USA; and* [2]*Department of Genetics, Perelman School of Medicine, University of Pennsylvania, Philadelphia, Pennsylvania, USA*

[3]*These authors contributed equally to this work.*

Correspondence: Yana G. Kamberov, Department of Genetics, Perelman School of Medicine, University of Pennsylvania, 415 Curie Boulevard, Philadelphia, Pennsylvania 19104-6145, USA. E-mail: yana2@pennmedicine.upenn.edu

Abbreviations: EDA, ectodysplasin; XLHED, X-linked hypohidrotic ectodermal dysplasia

Received 2 June 2022; revised 4 January 2023; accepted 2 February 2023; accepted manuscript published online 18 February 2023; corrected proof published online 27 March 2023

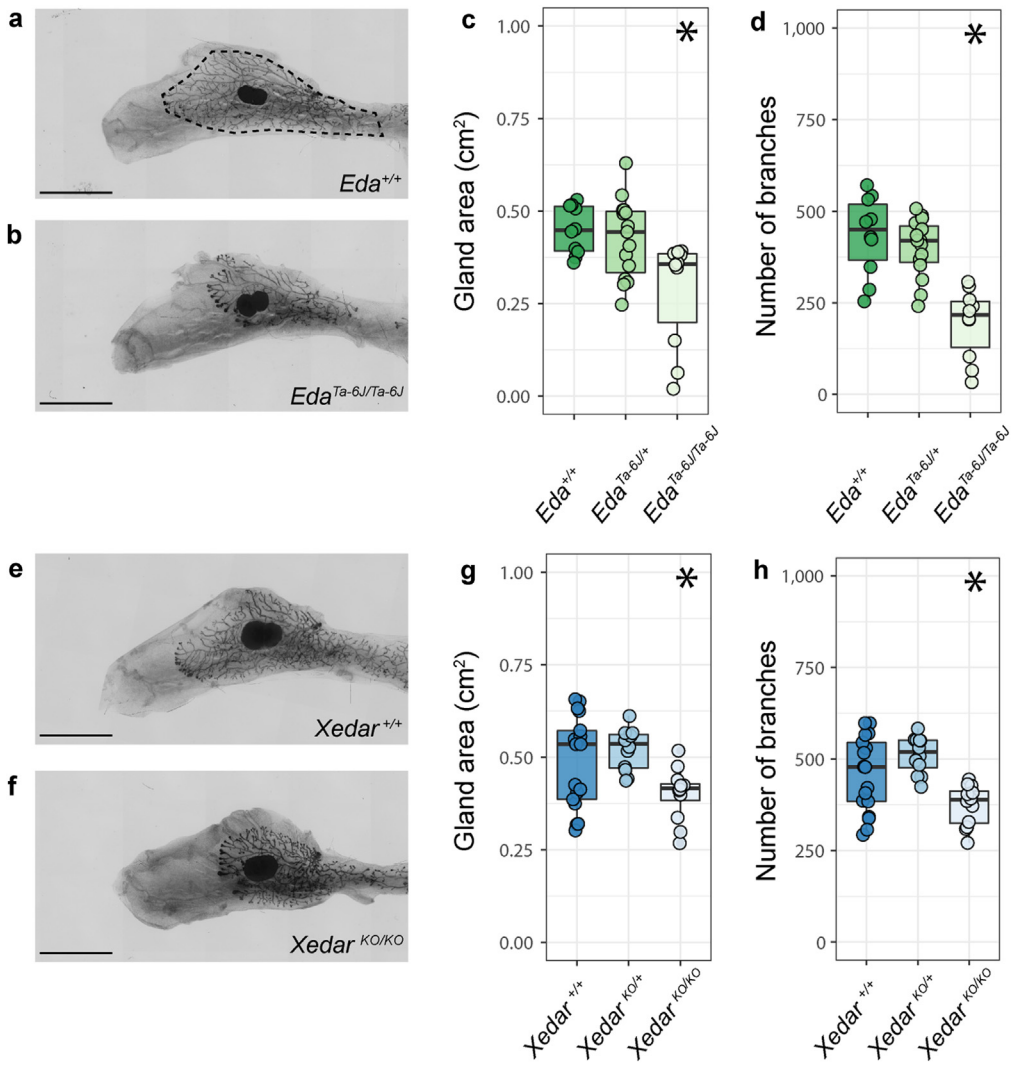

Figure 1. *Xedar* is required for the development of *Eda*-dependent mammary epithelial traits. (**a, b**) Representative images of the fourth inguinal mammary gland from virgin female mice aged 6 weeks of designated *Eda* genotypes on C57BL/6J genetic background (+ denotes wild type allele). The dotted line indicates the gland area. (**c**) Area of the mammary epithelial tree across *Eda* genotypes. (**d**) Epithelial branch count across *Eda* genotypes. (**e, f**) Representative images of the fourth inguinal mammary glands from virgin mice aged 6 weeks of designated *Xedar* genotypes on C57BL/6N genetic background (KO denotes knockout allele). (**g**) Area of the mammary epithelial tree across *Xedar* genotypes. (**h**) Epithelial branch count across *Xedar* genotypes. Boxplots show the median and quartile distributions for genotype categories. Dots represent phenotype values for individual mice analyzed in these experiments. Asterisks indicate $P < 0.05$ by Kruskal–Wallis testing. Bar = 5 mm. EDA, ectodysplasin.

In humans, XLHED-inducing sequence variants generally result in dysfunction or loss of both EDA-A1 and EDA-A2 isoforms, as do the $Eda^{Ta\text{-}6J}$ and Eda^{Ta} mouse mutations (Cluzeau et al., 2011; Wohlfart et al., 2016). Accordingly, deciphering the individual roles of the two ligand isoforms in ectodermal appendage biology relies on the characterization of the effects of the receptors that mediate signaling by EDA-A1 and EDA-A2, respectively, namely EDAR and XEDAR. However, unlike the dramatic ectodermal appendage phenotypes resulting from *Edar* loss-of-function mutations, *Xedar*-knockout ($Xedar^{KO}$) mice are reported to have normal hair, eccrine gland, and tooth development (Newton et al., 2004). Moreover, ectopic expression of an EDA-A2 transgene or recombinant Fc-EDA-A2 does not rescue hair, eccrine, or tooth phenotypes in *Eda*-mutant mice, underscoring the importance of the EDA-A1/EDAR pathway in the development of this subset of ectodermal appendages (Casal et al., 2007; Gaide and Schneider, 2003; Margolis et al., 2019).

Analyses of the mammary glands of $Xedar^{KO}$ mice have not been reported. The mammary gland and its supporting structures are of clinical importance in humans because the majority of female XLHED carriers report lactation difficulties (Clarke et al., 1987). This is notable because the treatment with or ectopic expression of EDA-A1 improves but does not fully rescue the mammary phenotypes of mouse *Eda* mutants, including the reduction of mammary gland branching and lactation deficits (Mustonen et al., 2003; Srivastava et al., 2001; Wahlbuhl et al., 2018). In light of these observations and motivated by the clinical need to fully understand the etiology of human XLHED mammary phenotypes, we investigated the phenotypic consequences of disrupting the EDA-A2/XEDAR signaling axis on mammary gland morphogenesis using a constitutive $Xedar^{KO}$ mouse model.

RESULTS AND DISCUSSION

The loss of *Xedar* disrupts *Eda*-dependent epithelial mammary gland phenotypes

To establish a baseline spectrum of *Eda*-sensitive mammary phenotypes and to quantify the magnitude of effects of *Eda* loss on these traits, we evaluated two primary mammary traits previously reported to be attenuated in *Eda*-mutant females, namely the size of the mammary gland (measured as the area invaded by the mammary epithelium into the mammary fat pad stroma) and the extent of branching of the mammary ductal tree (Chang et al., 2009; Voutilainen et al., 2012;

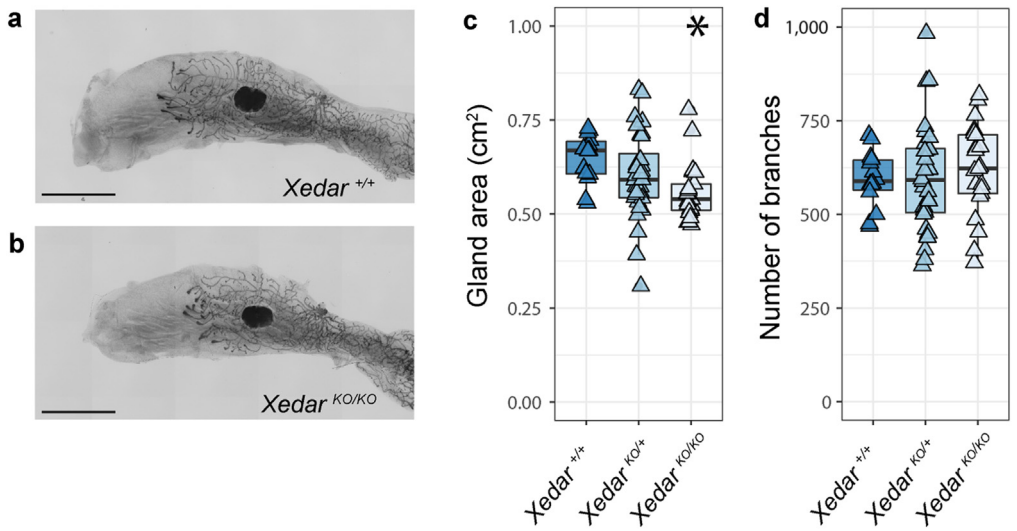

Figure 2. *Xedar* is necessary for postpubertal mammary epithelial growth but not branching on an FVB/N genetic background. (**a, b**) Representative images of the fourth inguinal mammary gland of virgin, N4FVB/N female mice aged 6 weeks of the designated *Xedar* genotypes. (**c**) Area of the mammary epithelial tree across *Xedar* genotypes (+ denotes wild type allele; KO denotes knockout allele). (**d**) The number of epithelial branches within the mammary gland across *Xedar* genotypes. Boxplots show the median and quartile distributions in each genotype category. Triangles represent phenotype values for individual mice analyzed in these experiments. Asterisks indicate $P < 0.05$ by Kruskal–Wallis tests. Bar = 5 mm.

Wahlbuhl et al., 2018) (Figure 1a–d). Analyses of the left and right fourth inguinal mammary glands of virgin female mice aged 6 weeks confirm significant decreases in both gland area and branching in $Eda^{Ta\text{-}6J}$ homozygotes compared with that in heterozygous and wild type females on a C57BL/6J genetic background (Figure 1a–d and Supplementary Table S1) ($\chi^2 = 9.26[2]$, $P < 0.05$ and $\chi^2 = 17.9[2]$, $P < 0.05$, respectively). Because mammary branching increases with body size in C57BL/6 substrains (Supplementary Figure S1) and $Eda^{Ta\text{-}6J}$ mice are smaller than their littermates (Supplementary Table S1) ($\chi^2 = 10.5[2]$, $P < 0.05$), we confirmed that the disruption of branching that occurs with the loss of EDA signaling persists when branching is scaled by body size (Supplementary Table S1) (branches per gram; $\chi^2 = 17.6[2]$, $P < 0.05$). The effect of *Eda* on mammary morphogenesis appears to be restricted to the epithelium because we do not find an effect of *Eda* disruption on the area of the mammary stroma or fat pad (Supplementary Tables S1) ($\chi^2 = 2.31[2]$, $P = 0.315$).

Disruption of *Xedar* in C57BL/6N female mice affects both *Eda*-sensitive mammary gland traits. $Xedar^{KO}$ female mice exhibit reduced epithelial gland area and branching compared with wild-type and hemizygous $Xedar^{KO}$ females (Figure 1e–h and Supplementary Table S1) ($\chi^2 = 9.41[2]$, $P < 0.05$ and $\chi^2 = 13.2[2]$, $P < 0.05$, respectively). As with the loss of *Eda*, the effect of *Xedar* disruption is still observed when branching is scaled to body weight (Supplementary Table S1) ($\chi^2 = 18.5[2]$, $P < 0.05$) and is restricted to the epithelium with no effect on the fat pad area (Supplementary Table S1) ($\chi^2 = 0.19[2]$, $P = 0.906$).

Because the C57BL/6J and C57BL/6N substrains show comparable baseline branching and gland size phenotypes (Figure 1a–h), we could qualitatively compare the effects of disrupting the *Eda* and *Xedar* receptors on each of these mammary characteristics. Disrupting each gene results in a reduction of epithelial growth and branching. Branching is more severely attenuated with the loss of *Eda* than with the loss of *Xedar*, suggesting that *Eda* is able to support some branching in the absence of *Xedar*. Nevertheless, our data implicate *Xedar* in the differentiation of the adult mammary tree and provide direct evidence that *Xedar* affects *Eda*-dependent ectodermal appendage phenotypes.

The effect of *Xedar* on mammary epithelial traits is dependent on genetic background

The patterns of growth and branching of the mammary epithelium vary among mouse strains (Gardner and Strong, 1935; Naylor and Ormandy, 2002). Nevertheless, the effect of *Eda* disruption has been reported across several mouse strains (Chang et al., 2009; Voutilainen et al., 2012). Indeed, we observe that disruption of *Eda* on an FVB/N strain background has consistent effects with those we observe in C57BL/6J mice (Supplementary Table S1). To determine whether *Xedar* loss showed similar phenotypic penetrance across genetic backgrounds, we examined the necessity of *Xedar* for normal mammary development in a second and genetically diverged laboratory mouse strain by backcrossing our $Xedar^{KO}$ allele onto FVB/N for at least four generations (N4) and compared the results with those of our C57BL/6N study (Lilue et al., 2018).

In virgin N4 FVB/N female mice aged 6 weeks, mammary glands are larger and more branched than those of C57BL/6N mice, even when accounting for the larger body size observed in the FVB/N strain (Supplementary Figure S2 and Supplementary Table S1). Mammary gland area is significantly affected by the *Xedar* genotype on an N4FVB/N background, with homozygous $Xedar^{KO}$ females having a reduced gland area compared with wild-type or hemizygous carriers (Figure 2a–c and Supplementary Table S1) ($\chi^2 = 10.0[2]$, $P < 0.01$). These data show that *Xedar* acts to promote the growth of the mammary epithelium on this genetic background, much as it does in the C57BL/6N strain. In contrast, disruption of *Xedar* does not affect the number of mammary branches in FVB/N mice (Figure 2a, b, and

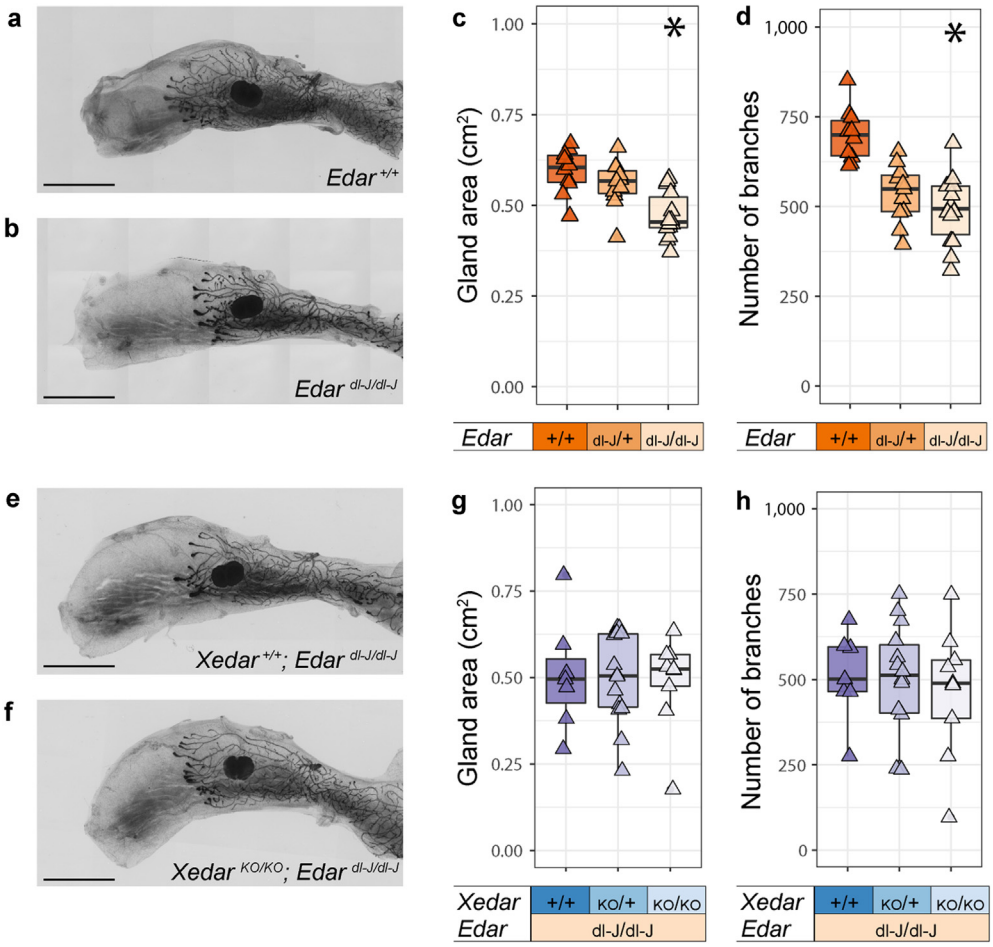

Figure 3. *Edar* is epistatic to *Xedar* in the regulation of postpubertal mammary epithelium. (**a, b**) Representative images of the fourth inguinal mammary glands of virgin female mice aged 6 weeks of the designated *Edar* genotypes (+ denotes wild type allele; dl-J denotes downless J $Edar^{dl\text{-}J}$ allele). (**c**) Area of the mammary epithelial tree across *Edar* genotypes. (**d**) The number of epithelial branches of the mammary gland across *Edar* genotypes. (**e, f**) Representative images of the fourth inguinal mammary glands of virgin female mice aged 6 weeks with compound disruptions in EDAR and XEDAR (KO denotes knockout allele). (**g**) Area of the mammary epithelial tree across the designated *Edar* and *Xedar* compound genotypes. (**h**) The number of epithelial branches of the mammary gland across the designated *Edar* and *Xedar* compound genotypes. Triangles represent phenotype values for individual mice analyzed in these experiments. Asterisks indicate $P < 0.05$ by Kruskal–Wallis tests. Bar = 5 mm. EDAR, ectodysplasin receptor; KO, knockout.

d and Supplementary Table S1: gland area) ($\chi^2 = 0.85[2]$, $P = 0.651$). We find that puberty proceeds normally in $Xedar^{KO}$ homozygous and hemizygous mice as measured by the day of estrous onset, indicating that systemic effects of altered puberty can be excluded as a possible cause for the phenotypes we observe (Supplementary Figure S3).

Xedar's ability to promote epithelial growth in two different mouse strains but to promote branching in a strain-specific manner suggests that genetic modifiers may influence the extent to which EDA-A2/XEDAR signaling contributes to *Eda*-dependent mammary phenotypes. These data suggest that genetic context may have a profound influence on the phenotypic implications of *Xedar* variants, particularly in diverse species such as humans.

Xedar loss does not potentiate *Edar*-dependent mammary defects

In light of our finding that *Xedar* affects mammary phenotypes known to be sensitive to the EDA-A1/EDAR signaling axis, we investigated whether *Xedar* and *Edar* may independently or redundantly mediate the effects of *Eda* on mammary epithelial growth and branching. To this end, we analyzed mammary gland phenotypes in mice carrying the classical downless J *Edar* allele ($Edar^{dl\text{-}J}$), which was previously reported to encode a recessive EDAR variant responsible for producing hypohidrotic/anhidrotic ectodermal dysplasia–like phenotypes in the mouse (Chang et al., 2009; Headon and Overbeek, 1999). Consistent with previous reports, gland areas and branch numbers are significantly reduced in the mammary glands of virgin female mice aged 6 weeks homozygous for the $Edar^{dl\text{-}J}$ mutation (Figure 3a–d and Supplementary Table S1) ($\chi^2 = 14.2[2]$, $P < 0.05$ and $\chi^2 = 18.5[2]$, $P < 0.05$ for gland area and branching, respectively). Notably, $Edar^{dl\text{-}J}$ heterozygotes are intermediate in branch number between wild type controls and homozygotes, highlighting the sensitivity of this phenotype to EDA-A1/EDAR signaling (Figure 3d). This finding is consistent with the growing evidence that *Edar* is haploinsufficient for a subset of ectodermal appendage phenotypes (Kamberov et al., 2013).

By intercrossing $Edar^{dl\text{-}J}$ mice with $Xedar^{KO}$ mice, we generated females that are homozygous for the $Edar^{dl\text{-}J}$ mutation and either wild type, hemizygous, or homozygous for the $Xedar^{KO}$ allele. Analysis of mammary gland area and branch number in these mice does not reveal any effect of the loss of *Xedar* beyond the loss of *Edar* alone (Figure 3e–h and Supplementary Table S1) ($\chi^2 = 0.22[2]$, $P = 0.892$ and $\chi^2 = 0.22[2]$, $P = 0.895$).

The failure of *Xedar* disruption to potentiate *Edar*-dependent mammary phenotypes suggests that although *Xedar* and *Edar* can function independently, *Edar* is epistatic to *Xedar* in the regulation of mammary epithelial differentiation and growth. This may reflect a difference in the timing during which the two receptors regulate mammary morphogenesis or a difference in the downstream signaling mechanism

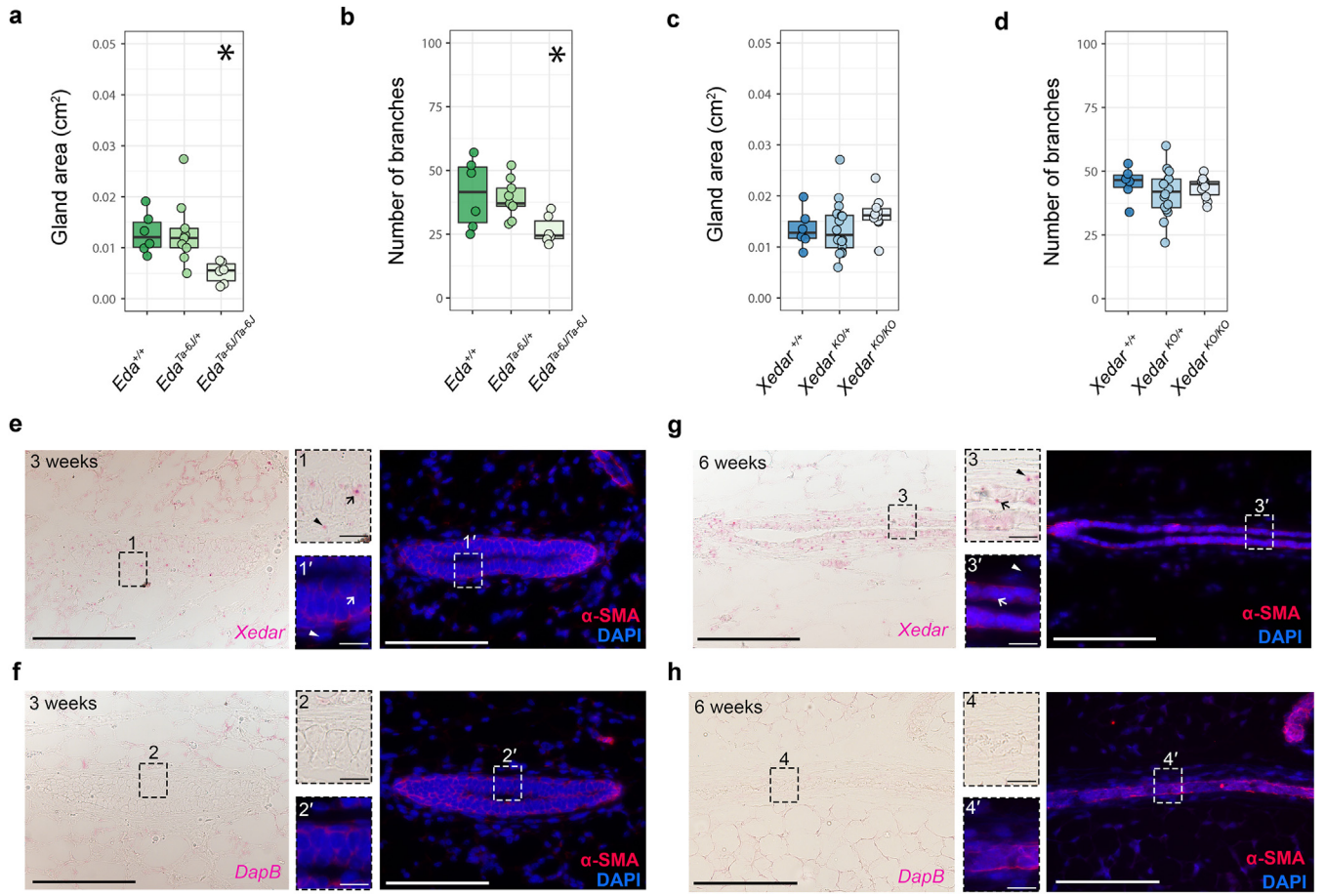

Figure 4. Spatiotemporal specificity of *Xedar* in mammogenesis. (**a**−**d**) Assessment of the fourth inguinal mammary gland characteristics in virgin wild type, *Eda*-variant, and *Xedar*-variant mice aged 3 weeks. Area of the (**a**) mammary epithelial tree and (**b**) branch count in wild type, hemizygous, and homozygous $Eda^{Ta\text{-}6J}$ female mice aged 3 weeks (+ denotes wild type allele). Area of the (**c**) mammary epithelial tree and (**d**) branch count in mammary glands of wild type, hemizygous, and homozygous $Xedar^{KO}$ female mice (KO denotes knockout allele). Dots and whiskers show the median and quartiles. Asterisks indicate $P < 0.05$ by Kruskal−Wallis tests. (**e**−**h**). *Xedar* mRNA expression in the fourth inguinal mammary glands of female mice at (**e**) 3 and (**g**) 6 weeks. *Xedar* expression is visualized using RNAscope detection (red dots, brightfield image panels). Sections were counterstained with α-SMA (red) antibody to detect basal myoepithelial cells and DAPI (blue) to visualize the nuclei (fluorescent, darkfield panels). Arrow denotes the basal myoepithelial cells; arrowheads denote the mesenchymal cells of the mammary fat pad. (**f, h**) RNAscope detection with the negative control dapB probes (red dots denotes brightfield image panels) of virgin female mice aged 3 (**f**) and 6 (**h**) weeks. Magnified images corresponding to the boxed regions of each image are shown. Main panels bar = 0.1 mm; insets bar = 0.010 mm. α-SMA, α-smooth muscle actin.

engaged by each branch of the *Eda* pathway in this context. Previous studies have implicated NFkB as the major mediator of EDA-A1/EDAR signaling in mammary gland development, raising the possibility that in the context of the mammary gland, XEDAR functions through alternative signaling mediators, such as c-Jun N-terminal kinase signaling (Kumar et al., 2001; Lindfors et al., 2013; Sinha et al., 2002; Voutilainen et al., 2015). Thus, our results suggest that multiple mechanisms may converge to regulate the mammary epithelial tree downstream of *Eda*.

Xedar effects on mammary gland differentiation are temporally restricted

The development and differentiation of the mammary epithelium occur in distinct stages, beginning in mid-embryogenesis and continuing into adulthood (McNally and Martin, 2011; Myllymäki and Mikkola, 2019; Watson and Khaled, 2008). Consistent with previous reports, we find that branching and size of the epithelial mammary tree are significantly reduced not only during the late pubertal period but also in prepubertal homozygous $Eda^{Ta\text{-}6J}$ mice at age 3 weeks (Figure 4a and b) (gland area: $\chi^2 = 10.2[2]$, $P < 0.05$; branches: $\chi^2 = 7.66[2]$, $P < 0.05$) (Chang et al., 2009; Lindfors et al., 2013; Voutilainen et al., 2015, 2012). In contrast, we do not observe significant differences in mammary gland area or epithelial branch number in female mice aged 3 weeks carrying zero, one, or two copies of the $Xedar^{KO}$ allele (Figure 4c and d) (gland area: $\chi^2 = 2.15[2]$, $P = 0.341$; branches: $\chi^2 = 1.58[2]$, $P = 0.452$). These data contrast with the effects of *Edar* disruption, which alters gland development at multiple stages, including embryonically and during the prepubertal period (Lindfors et al., 2013; Voutilainen et al., 2015, 2012). Instead, *Xedar*'s effects are temporally restricted to the stage when hormonal cues provide the major directives for gland maturation. This is intriguing given that *Xedar* expression is evident in the mammary epithelium and in the mammary stroma at this stage and also during embryonic stages of mammogenesis

(Figure 4e and f and Supplementary Figure S4). The expression of *Xedar* persists at 6 weeks, the stage when *Xedar*-dependent phenotypes are evident in the gland. At this stage, we detect *Xedar* transcripts in both the basal myoepithelial cells of the mammary gland, which also express the marker α-smooth muscle actin, and in the surrounding mesenchyme (Figure 4g and h) (Deugnier et al., 1995; Haaksma et al., 2011). Because mammogenesis requires reciprocal signaling between the gland and the mesenchyme, these data raise the possibility that XEDAR may mediate EDA-A2 effects on mammary growth by both direct and indirect signaling to the mammary gland itself (Watson and Khaled, 2008).

The temporal restriction of the $Xedar^{KO}$ mammary phenotypes suggests a model in which *Xedar* and *Edar* differentially contribute to the regulation of mammary epithelial development and differentiation downstream of *Eda* at multiple stages of mammogenesis. In so doing, our findings point to a complex underlying basis for the effects of *Eda* on mammary glands. This may help to explain the incomplete rescue of mammary phenotypes in tabby mice by EDA-A1 alone and supports a contribution from the EDA-A2/XEDAR signaling axis in the etiology of mammary defects in human XLHED carriers. Given the dynamic nature of the mammary gland, which is subject to dramatic changes in growth, functionalization, and regression, future experiments are needed to understand whether *Xedar* contributes to *Eda*-dependent phenotypes in other contexts beyond the pubertal period. This is important because *EDA* loss of function is associated with persistent mammary phenotypes in both humans and mice (Cluzeau et al., 2011; Wahlbuhl et al., 2018). The generation of conditional alleles that enable temporal and tissue-specific disruption of *Xedar* would greatly enhance such efforts. These genetic tools would also make it possible to parse out whether *Xedar*-dependent mammary phenotypes are directly attributable to *Xedar* expression within one or more of the mammary tissues we report in this paper or are an indirect consequence of *Xedar* function in other tissues such as the skeletal muscle, where this gene is also highly expressed and influences systemic, metabolic phenotypes (Awazawa et al., 2017; Newton et al., 2004).

In a broader context, our study provides evidence implicating the EDA-A2/XEDAR signaling axis in the regulation of ectodermal appendage phenotypes. Unlike the effects of other characterized components of the *Eda* pathway on ectodermal appendage traits, the effects of *Xedar* appear to be restricted to the mammary gland (Newton et al., 2004). Our finding that *Xedar*'s effects on the mammary gland can be sensitive to genetic background is noteworthy given that a derived *XEDAR* coding variant (XEDAR R57K, rs1385699) is highly differentiated among modern humans and was computationally identified as a potential target of positive natural selection in East Asia (Sabeti et al., 2007). Intriguingly, we have previously reported that a strongly selected coding variant of *EDAR* (EDARV370A, rs3827760) that is prevalent in present-day East Asian populations has pleiotropic effects on a subset of *EDA*-dependent ectodermal appendage traits, including mammary gland branching (Kamberov et al., 2013). Thus, our findings raise the possibility that an additional *EDA* pathway effector, *XEDAR*, may also contribute to evolutionarily significant differences in mammary epithelial traits among modern humans.

MATERIALS AND METHODS

Experimental mice

Mice were housed in groups (up to five mice per cage) on a 12-hour light–dark cycle with continuous access to food and water. Pups were weaned at 3 weeks and raised thereafter in single-sex groups. All experimental procedures were conducted in accordance with regulations and approvals by the Harvard Medical School (Boston, MA), the Perelman School of Medicine Institutional Animal Care and Use Committees (Philadelphia, PA), and the National Institutes of Health Guide for the Care and Use of Laboratory Animals.

Mouse lines

Xedar-deficient mice (*Xedar* knockout [$Xedar^{KO}$] mice) have been previously described (Newton et al., 2004) and were obtained under material transfer agreement (number OM-212731) from Genentech (South San Francisco, CA). $Xedar^{KO}$ mice harbor a targeted disruption in exon 4 of the *Xedar* locus, leading to the deletion of the XEDAR transmembrane domain and a nonfunctional protein (Newton et al., 2004). $Xedar^{KO}$ mice were obtained on a C57BL/6N genetic background and were maintained on C57BL/6N by further backcrossing to C57BL/6NTac (Taconic Biosciences, Germantown, NY) mice. In addition, $Xedar^{KO}$ mice were separately backcrossed onto FVB/NCrl (Charles River Laboratories, Wilmington, MA) for at least four generations for analyses pertaining to the effects of genetic background on mammary phenotypes. *Eda* tabby 6J ($Eda^{Ta\text{-}6J}$) mice (JAX stock number 000338, Jackson Laboratory, Bar Harbor, ME, $A^{w\text{-}J}$-$Eda^{Ta\text{-}6J}$/J) (Srivastava et al., 1997) harboring a base pair deletion (at position 1049) in *Eda* that results in a frameshift mutation and the production of a nonfunctional, truncated protein were maintained on a C57BL/6J background (C57BL/6J, Jackson Laboratory) and backcrossed onto FVB/NCrl (Charles River Laboratories) for four generations to examine strain effects. Edar downless J ($Edar^{dl\text{-}j}$) mutant mice were previously described (Headon and Overbeek, 1999) and obtained from Jackson Laboratories (JAX stock number 000210, B6C3Fea/*a*-$Edar^{dl\text{-}J}$/J) and were backcrossed onto FVB/NCrl for at least eight generations before analyses.

To examine whether *Xedar* deficiency could potentiate mammary phenotypes in the context of diminished EDAR signaling, we created mice with compound homozygous deficiencies in *Xedar* and *Edar* on an FVB/N background. These lines were separately backcrossed to FVB/NCrl (Charles River Laboratories) for four and eight generations, respectively, before the intercross. Experimental mice were either agouti or albino. All the mice analyzed in the compound test crosses were $Edar^{dl\text{-}J/dl\text{-}J}$ and showed symptoms of ectodermal dysplasia, including a thin coat and a hairless, kinked tail.

Genotyping

$Xedar^{KO}$ mice were genotyped using the following primers: for Xedar-1, 5′-tcgcaggactatgattgctaggc; for Xedar-2, 5′-gccatctgcatcaggtttcctatc; for Xedar-3, 5′- aggaaggcccattatcatgcagtc; and for Xedar-4, 5′-ccagaggccacttgtgtagcg. The resulting PCR products are distinguishable by size using gel electrophoresis (wild type band: 616 bp; mutant band: 302 bp).

$Edar^{dl\text{-}J}$ mice carry a mutation in the ectodysplasin receptor that results in G/A substitution (5′gtgaaaacatggcgccaccttgcc $G^{(wt)}/A^{(dl\text{-}J)}$ agagctttggactgaag3′) in the *Edar* locus and an E379K amino acid change (Headon and Overbeek, 1999). The *dl-J* mutation was genotyped by sequencing the PCR product using the primers 5′-gtctcagccccaccgagttg for (dl(J) forward and 5′-gtggggaggcaggtggtaca for dl(J) reverse to amplify genomic DNA from mouse tail biopsies. Tabby homozygote ($Eda^{Ta\text{-}6J/Ta\text{-}6J}$), hemizygote ($Eda^{wt/Ta\text{-}6J}$), and wild type mice can be

readily distinguished by eye when bred on a pigmented strain. Homozygotes exhibit ectodermal dysplasia hair phenotypes, and heterozygotes have a striped tabby coat. To allow our $Eda^{Ta\text{-}6J}$ heterozygotes to be visually genotyped on the FVB/N background (which is not possible in an albino), we maintained the line with an $A^{w\text{-}J}$ agouti allele.

Tissue preparation

The fourth and fifth inguinal mammary glands and associated fat pads were dissected from virgin female mice aged 3 and 6 weeks, respectively. Whole-mount mammary preparations were made as follows: glands were fixed flat in Carnoy's fixative (six parts ethanol, three parts chloroform, and one part glacial acetic acid) for 2 hours at room temperature and stored in 70% ethanol. After rehydration, glands were stained overnight with Carmine alum solution (1 g carmine, C1022, Sigma-Aldrich, St. Louis, MO, with 2.5 g aluminum potassium sulfate A7167, Sigma-Aldrich, to 500 ml with distilled water, boiled, and filtered). Stained glands were dehydrated, cleared in xylenes, flat mounted on glass slides, and imaged in brightfield with an Olympus VS120 slide scanner microscope.

Analysis of mammary phenotypes

Mammary phenotypes were assessed using digital images analyzed in FIJI (ImageJ, National Institutes of Health, Bethesda, MD) with the Bioformats importer (Schindelin et al., 2012). Automatic branch counting was tested but was not as accurate as manual counting. Therefore, ductal termini (branch tips) were counted manually using the FIJI Cell Counter plugin. Images were blindly analyzed at least two times to ensure the accuracy and reproducibility of measurements. Fat pad area was measured from the main lactiferous duct to the dorsolateral border. Gland length was measured from the distal-most ductal termini at the dorsal and ventral edges of the gland, capturing the maximum bidirectional growth of the ductal tissue area across the fat pad. Gland area was measured by capturing the area invaded by the mammary epithelium from branch tip to tip across the extent of the mammary fat pad (Figure 1). Left and right fourth mammary gland counts and measurements were averaged for each individual in all experiments except the *Xedar*−*Edar* compound cross and the developmental series, for which only the left glands were used.

Determination of estrus onset

Beginning on postnatal day 20, the vaginas of virgin, female mice (FVB/N background and hemizygous or homozygous for the $Xedar^{KO}$ allele) were observed daily, and the day of estrus onset was tabulated, as described earlier (Ajayi and Akhigbe, 2020). The data reported were obtained from females from two different litters.

Statistics

Statistical analyses were performed in R Statistical Software (version 4.1.2) (R Core Team, 2022). Mammary characteristics were compared using Kruskal−Wallis nonparametric tests because the normality requirements of parametric analysis were not met for all distributions in the dataset. Parametric and nonparametric analyses gave the same qualitative results in 94.7% of tests performed.

A minimum of 10 females from each genotype class were used in all comparisons except in the compound *Xedar*−*Edar* experiment, for which only seven *Xedar* wild type and nine $Xedar^{KO/KO}$; $Edar^{dl\text{-}J/dl\text{-}J}$ compound mutant mice could be acquired. For our strain comparison, wild type mice from all mouse lines were combined, resulting in 27 C57BL/6N and 34 FVB/N wild type mice. This information is available in Supplementary Table S1.

The significance of differences in estrus timing between $Xedar^{KO}$ hemizygous and homozygous knockout female mice was assessed by an unpaired, two-tailed Student's *t*-test.

In situ hybridization

CD1/NCrl (Charles River Laboratories) embryos were harvested on embryonic day 13.5, fixed overnight with 4% paraformaldehyde in 1 × PBS, and cryosectioned at 10 μm. The fourth inguinal mammary gland was dissected from CD1/NCrl virgin female mice aged 3 or 6 weeks, fixed overnight in 10% neutral-buffered formalin, and embedded in parafilm for posterior sectioning at 10 μm. RNAscope assay was performed as per the manufacturer's instructions for fixed, frozen, or formalin-fixed paraffin-embedded tissue and using RNAscope 2.5 Chromogenic assay reagent kit (Advanced Cell Diagnostics, Newark, CA). The *Xedar* (ACD: 531871) and the negative control dapB (ACD: 310043) probes were designed by ACD. Targeted regions for *Xedar* and dapB probes were 304 bp− 1,253 bp and 414 bp−862 bp in the transcript, respectively. Immunofluorescent staining to detect keratin 14 or α-smooth muscle actin was performed after RNAscope detection on the same tissue sections. The keratin 14 antibody detects the basal keratinocyte layer of the ectoderm, which includes the cells of the developing mammary gland, which are also derivatives of this layer. The α-smooth muscle actin antibody detects basal myoepithelial cells derived from the basal keratinocyte layer of the developing mammary gland. Histological sections were prepared through the developing mammary bud and through muscle, in which *Xedar* was previously reported to be expressed (Awazawa et al., 2017; Newton et al., 2004). Briefly, samples were washed in PBS and blocked in PBS + 0.1% Tween + 10% normal donkey serum before overnight incubation in Cytokeratin 14 primary antibody (PRP155-P CK14, 1:10,000, Covance, Princeton, NJ) or α-smooth muscle actin. Samples were washed in PBS + 0.1% Tween and incubated with Alexa Fluor^{488} (1:250, Jackson ImmunoResearch, West Grove, PA) or Alexa Fluor^{647} (1:250, Abcam, Waltham, MA) and DAPI (1:5,000, Sigma-Aldrich). Images were acquired on a Leica DM5500 microscope equipped with a Leica DEC500 camera.

Data availability statement

All the data analyzed in this study are reported in the manuscript. All mouse strains analyzed in this study have been previously published and are available from the vendors and sources listed in the Materials and Methods.

ORCIDs

Abigail R. Wark: http://orcid.org/0000-0002-4760-5627
Daniel Aldea: http://orcid.org/0000-0001-5101-0194
Reiko R. Tomizawa: http://orcid.org/0000-0002-9993-0325
Blerina Kokalari: http://orcid.org/0000-0003-1037-6901
Bailey Warder: http://orcid.org/0000-0002-2375-6498
Yana G. Kamberov: http://orcid.org/0000-0002-6239-1831

CONFLICT OF INTEREST

The authors state no conflict of interest.

ACKNOWLEDGMENTS

We thank Clifford J. Tabin for resources in support of this study (Eunice Kennedy Shriver National Institute of Child Health & Human Development of the National Institutes of Health Award R01HD032443). We also thank Joseph Patrice and Parimal Rana for excellent animal care. We thank Genentech for sharing the *Xedar*-knockout mouse model (number OM-212731). We thank the Penn Biology and Diseases Resource-based Center Core A (P30-AR069589) and the Harvard Medical School NeuroImaging Facility with support from the Neural Imaging Center (P30-NS072030). The research reported in this publication was supported by a National Institute of Arthritis Musculoskeletal and Skin Diseases of the National Institutes of Health Award

R01AR077690 and a National Science Foundation BCS-1847598 award to YGK.

AUTHOR CONTRIBUTIONS

Conceptualization: ARW, YGK; Formal Analysis: ARW, DA, RRT; Funding Acquisition: YGK; Investigation: ARW, DA, RRT, BK, BW; Methodology: ARW, DA; Resources: YGK; Supervision: YGK; Validation: ARW; Visualization: ARW, DA; Writing - Original Draft Preparation: ARW, YGK; Writing - Review and Editing: ARW, DA, YGK

Disclaimer

Any opinions, findings, and conclusions or recommendations expressed in this material are those of the authors and do not necessarily reflect the views of the National Science Foundation. The content is solely the responsibility of the authors and does not necessarily represent the official views of the National Institutes of Health.

SUPPLEMENTARY MATERIAL

Supplementary material is linked to the online version of the paper at www.jidonline.org, and at https://doi.org/10.1016/j.jid.2023.02.007

REFERENCES

Ajayi AF, Akhigbe RE. Staging of the estrous cycle and induction of estrus in experimental rodents: an update. Fertil Res Pract 2020;6:5.

Awazawa M, Gabel P, Tsaousidou E, Nolte H, Krüger M, Schmitz J, et al. A microRNA screen reveals that elevated hepatic ectodysplasin A expression contributes to obesity-induced insulin resistance in skeletal muscle. Nat Med 2017;23:1466–73.

Biggs LC, Mikkola ML. Early inductive events in ectodermal appendage morphogenesis. Semin Cell Dev Biol 2014;25–26:11–21.

Casal ML, Lewis JR, Mauldin EA, Tardivel A, Ingold K, Favre M, et al. Significant correction of disease after postnatal administration of recombinant ectodysplasin A in canine X-linked ectodermal dysplasia. Am J Hum Genet 2007;81:1050–6.

Chang SH, Jobling S, Brennan K, Headon DJ. Enhanced Edar signalling has pleiotropic effects on craniofacial and cutaneous glands. PLoS One 2009;4:e7591.

Clarke A, Sarfarazi M, Thomas NS, Roberts K, Harper PS. X-linked hypohidrotic ectodermal dysplasia: DNA probe linkage analysis and gene localization. Hum Genet 1987;75:378–80.

Cluzeau C, Hadj-Rabia S, Jambou M, Mansour S, Guigue P, Masmoudi S, et al. Only four genes (EDA1, EDAR, EDARADD, and WNT10A) account for 90% of hypohidrotic/anhidrotic ectodermal dysplasia cases. Hum Mutat 2011;32:70–2.

Cui CY, Kunisada M, Esibizione D, Douglass EG, Schlessinger D. Analysis of the temporal requirement for Eda in hair and sweat gland development. J Invest Dermatol 2009;129:984–93.

Cui CY, Schlessinger D. EDA signaling and skin appendage development. Cell Cycle 2006;5:2477–83.

Cui CY, Yin M, Sima J, Childress V, Michel M, Piao Y, et al. Involvement of Wnt, Eda and Shh at defined stages of sweat gland development. Development 2014;141:3752–60.

Deugnier MA, Moiseyeva EP, Thiery JP, Glukhova M. Myoepithelial cell differentiation in the developing mammary gland: progressive acquisition of smooth muscle phenotype. Dev Dyn 1995;204:107–17.

Gaide O, Schneider P. Permanent correction of an inherited ectodermal dysplasia with recombinant EDA. Nat Med 2003;9:614–8.

Gardner WU, Strong LC. The normal development of the mammary glands of virgin female mice of ten strains varying in susceptibility to spontaneous neoplasms. Am J Cancer 1935;25:282–90.

Haaksma CJ, Schwartz RJ, Tomasek JJ. Myoepithelial cell contraction and milk ejection are impaired in mammary glands of mice lacking smooth muscle alpha-actin. Biol Reprod 2011;85:13–21.

Headon DJ, Emmal SA, Ferguson BM, Tucker AS, Justice MJ, Sharpe PT, et al. Gene defect in ectodermal dysplasia implicates a death domain adapter in development. Nature 2001;414:913–6.

Headon DJ, Overbeek PA. Involvement of a novel Tnf receptor homologue in hair follicle induction. Nat Genet 1999;22:370–4.

Kamberov YG, Wang S, Tan J, Gerbault P, Wark A, Tan L, et al. Modeling recent human evolution in mice by expression of a selected EDAR variant. Cell 2013;152:691–702.

Kumar A, Eby MT, Sinha S, Jasmin A, Chaudhary PM. The ectodermal dysplasia receptor activates the nuclear factor-κB, JNK, and cell death pathways and binds to ectodysplasin A*. J Biol Chem 2001;276:2668–77.

Lilue J, Doran AG, Fiddes IT, Abrudan M, Armstrong J, Bennett R, et al. Sixteen diverse laboratory mouse reference genomes define strain-specific haplotypes and novel functional loci. Nat Genet 2018;50:1574–83.

Lindfors PH, Voutilainen M, Mikkola ML. Ectodysplasin/NF-κB signaling in embryonic mammary gland development. J Mammary Gland Biol Neoplasia 2013;18:165–9.

Margolis CA, Schneider P, Huttner K, Kirby N, Houser TP, Wildman L, et al. Prenatal treatment of X-linked hypohidrotic ectodermal dysplasia using recombinant ectodysplasin in a canine model. J Pharmacol Exp Ther 2019;370:806–13.

McNally S, Martin F. Molecular regulators of pubertal mammary gland development. Ann Med 2011;43:212–34.

Mikkola ML, Thesleff I. Ectodysplasin signaling in development. Cytokine Growth Factor Rev 2003;14:211–24.

Mustonen T, Ilmonen M, Pummila M, Kangas AT, Laurikkala J, Jaatinen R, et al. Ectodysplasin A1 promotes placodal cell fate during early morphogenesis of ectodermal appendages. Development 2004;131:4907–19.

Mustonen T, Pispa J, Mikkola ML, Pummila M, Kangas AT, Pakkasjärvi L, et al. Stimulation of ectodermal organ development by Ectodysplasin-A1. Dev Biol 2003;259:123–36.

Myllymäki SM, Mikkola ML. Inductive signals in branching morphogenesis – lessons from mammary and salivary glands. Curr Opin Cell Biol 2019;61:72–8.

Naylor MJ, Ormandy CJ. Mouse strain-specific patterns of mammary epithelial ductal side branching are elicited by stromal factors. Dev Dyn 2002;225:100–5.

Newton K, French DM, Yan M, Frantz GD, Dixit VM. Myodegeneration in EDA-A2 transgenic mice is prevented by XEDAR deficiency. Mol Cell Biol 2004;24:1608–13.

R Core Team. R: A Language and Environment for Statistical Computing. Vienna, Austria: R Foundation for Statistical Computing; 2022.

Sabeti PC, Varilly P, Fry B, Lohmueller J, Hostetter E, Cotsapas C, et al. Genome-wide detection and characterization of positive selection in human populations. Nature 2007;449:913–8.

Schindelin J, Arganda-Carreras I, Frise E, Kaynig V, Longair M, Pietzsch T, et al. Fiji: an open-source platform for biological-image analysis. Nat Methods 2012;9:676–82.

Schneider H, Faschingbauer F, Schuepbach-Mallepell S, Körber I, Wohlfart S, Dick A, et al. Prenatal correction of X-linked hypohidrotic ectodermal dysplasia. N Engl J Med 2018;378:1604–10.

Sinha SK, Chaudhary PM. Induction of Apoptosis by X-linked Ectodermal Dysplasia Receptor via a caspase 8-dependent Mechanism. J Biol Chem 2004;279:41873–81.

Sinha SK, Zachariah S, Quiñones HI, Shindo M, Chaudhary PM. Role of TRAF3 and -6 in the activation of the NF-κB and JNK pathways by X-linked ectodermal dysplasia receptor*. J Biol Chem 2002;277:44953–61.

Sofaer JA, MacLean CJ. Dominance in threshold characters. A comparison of two Tabby alleles in the mouse. Genetics 1970;64:273–80.

Srivastava AK, Durmowicz MC, Hartung AJ, Hudson J, Ouzts LV, Donovan DM, et al. Ectodysplasin-A1 is sufficient to rescue both hair growth and sweat glands in Tabby mice. Hum Mol Genet 2001;10:2973–81.

Srivastava AK, Pispa J, Hartung AJ, Du Y, Ezer S, Jenks T, et al. The Tabby phenotype is caused by mutation in a mouse homologue of the EDA gene that reveals novel mouse and human exons and encodes a protein (ectodysplasin-A) with collagenous domains. Proc Natl Acad Sci USA 1997;94:13069–74.

Tucker AS, Headon DJ, Schneider P, Ferguson BM, Overbeek P, Tschopp J, et al. Edar/Eda interactions regulate enamel knot formation in tooth morphogenesis. Dev Camb Engl 2000;127:4691–700.

Voutilainen M, Lindfors PH, Lefebvre S, Ahtiainen L, Fliniaux I, Rysti E, et al. Ectodysplasin regulates hormone-independent mammary ductal morphogenesis via NF-κB. Proc Natl Acad Sci USA 2012;109:5744–9.

Voutilainen M, Lindfors PH, Trela E, Lönnblad D, Shirokova V, Elo T, et al. Ectodysplasin/NF-κB promotes mammary cell fate via Wnt/β-catenin pathway. PLoS Genet 2015;11:e1005676.

Wahlbuhl M, Schuepbach-Mallepell S, Kowalczyk-Quintas C, Dick A, Fahlbusch FB, Schneider P, et al. Attenuation of mammary gland dysplasia and feeding difficulties in tabby mice by fetal therapy. J Mammary Gland Biol Neoplasia 2018;23:125–38.

Wahlbuhl-Becker M, Faschingbauer F, Beckmann MW, Schneider H. Hypohidrotic ectodermal dysplasia: breastfeeding complications due to impaired breast development. Geburtshilfe Frauenheilkd 2017;77:377–82.

Watson CJ, Khaled WT. Mammary development in the embryo and adult: a journey of morphogenesis and commitment. Development 2008;135:995–1003.

Wohlfart S, Hammersen J, Schneider H. Mutational spectrum in 101 patients with hypohidrotic ectodermal dysplasia and breakpoint mapping in independent cases of rare genomic rearrangements. J Hum Genet 2016;61:891–7.

Yan M, Wang LC, Hymowitz SG, Schilbach S, Lee J, Goddard A, et al. Two-amino acid molecular switch in an epithelial morphogen that regulates binding to two distinct receptors. Science 2000;290:523–7.

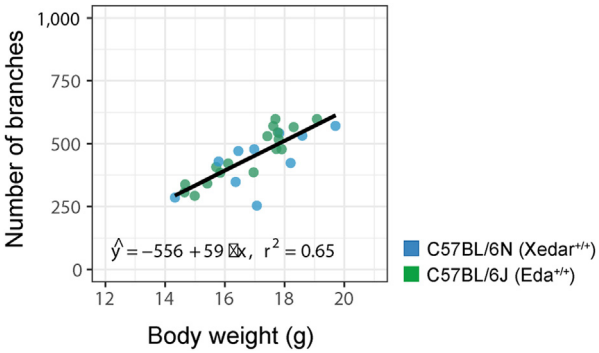

Supplementary Figure S1. Mammary branch number increases with body weight in substrains of C57BL/6. The epithelial branch number is plotted against body weight for individual wild type adult virgin females at age 6 weeks from C57BL/6N and C57BL/6J mouse substrains. Dots represent phenotype values for individual mice analyzed in these experiments.

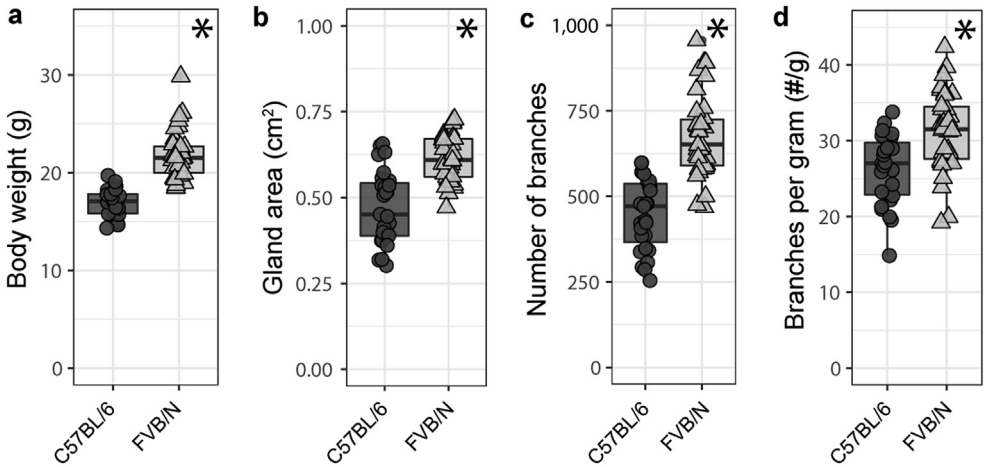

Supplementary Figure S2. Bodyweight and mammary characteristics are differentiated between mouse C57BL/6 substrain and FVB/N genetic backgrounds. (**a**–**d**) Characteristics of virgin wild type female mice aged 6 weeks from two genetic background categories: C57BL/6 (including C57BL/6N and C57BL/6J substrains) and FVB/N (including individuals that are four to eight generations backcrossed to FVB/N). Dots and triangles represent phenotype values for individual mice analyzed in these experiments, including (**a**) body weight in grams, (**b**) mammary epithelial tree area, (**c**) the number of epithelial branches, and (**d**) the number of branches scaled to body weight. Boxplots show the median and quartile ranges for each characteristic. Asterisks indicate $P < 0.05$ by Kruskal–Wallis tests. EDA, ectodysplasin.

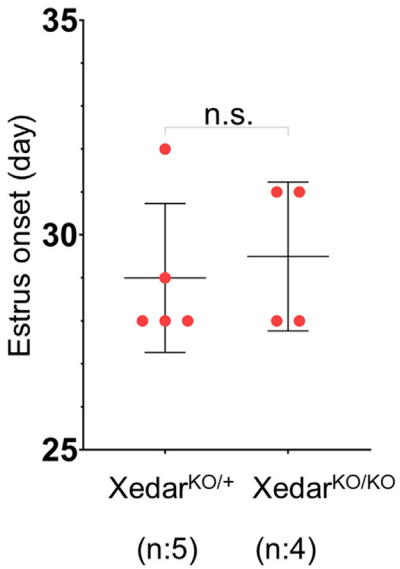

Supplementary Figure S3. Onset of estrus is not distinguished between hemizygous or homozygous *Xedar*^{KO} mice. The plot indicates the day of estrus onset. Each dot represents one independent observation in an individual mouse of the given genotype. Significance is assessed by an unpaired, two-tailed *t*-test. KO, knockout; ns, not significant.

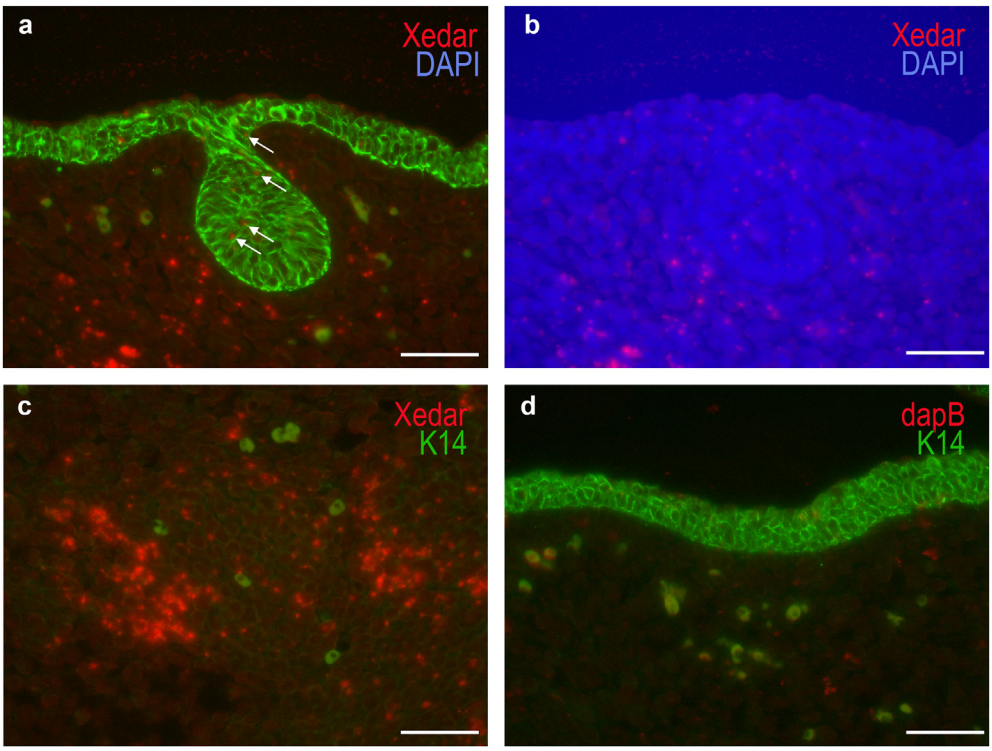

Supplementary Figure S4. *Xedar* expression during mammary development. In situ hybridization for *Xedar* mRNA (red dots), K14 protein (green), and DAPI nuclear stain (blue) in sections of mouse E13.5 (**a, b**) mammary bud and (**c**) muscle. White arrows denote positive *Xedar* signal. (**d**) In situ hybridization with negative control probe against dapB (red) in E13.5 skin section showing K14-positive basal keratinocytes. Bar = 0.05 mm. E13.5, embryonic day 13.5; K14, keratin 14; KO, knockout; n.s., not significant.